CHEMICAL ENGINEERING TRANSACTIONS
VOL. 90, 2022
A publication of AIDIC
The Italian Association of Chemical Engineering
Online at www.cetjournal.it
Guest Editors: Aleš Bernatík, Bruno Fabiano

ISBN 978-88-95608-88-4; **ISSN** 2283-9216
DOI: 10.3303/CET2290018

An Experimental and Numerical Study of the Blast Created by BLEVE of Superheated Water Contained in a Pipe

Frederic Heymes[a]*, Pol Hoorelbeke[b], Clement Chanut[a]

[a] Laboratoire des Sciences des Risques (LSR), IMT Mines Ales, Ales, France
[b] Total Energies, Paris, France
Frederic.heymes@mines-ales.fr

The blast created by a BLEVE is still a point of discussion; different considerations about the physics of BLEVE do not agree on the influence of flashing liquid on the pressure wave. In this work, a series of water BLEVE experiments was carried out in order to measure the internal pressure change and the aerial overpressure close to the vessel. Water was superheated at 290°C and contained in a tubular pipe with a rupture disk.
Data show two aerial pressure peaks; and show that pressure in the vessel remains quite constant during boiling. This could contribute to a piston effect entailing a pressure wave. However, experimental data doesn't demonstrate that this boiling plateau creates an overpressure. CFD modelling of the vapour release fits remarkably well with the overpressure data of the first peak. The second peak is not correctly represented by the vapour expansion modelling.

1. Introduction

A BLEVE is the explosive release of expanding vapour and boiling liquid when a container holding a pressure-liquefied gas fails catastrophically (Birk and Cunningham, 1994). The sudden pressure drop in the vessel can result in a violent release of expanded vapour and flashed liquid, creating several aerial overpressures and thermal radiation if the substance involved is flammable. Moreover, fragments and large pieces of the vessel can be ejected at a large distance.
Modelling the blast effect from a BLEVE has focused a large number of works. Diverse methods, such as the TNT-equivalence method, the pressure-burst-method by TNO and other scaling laws have been proposed previously (Li et al., 2020). More recently, the increase in the capacity of computers has fostered CFD modelling. It was shown that predictions are more accurate for far-field blast pressure prediction in free field (Van den Berg et al., 2006), (Yakush, 2016), (Li et al., 2020) and allow pressure wave calculation in obstructed areas or tunnel configurations (Li et al, 2021).
The main difficulty in CFD is to correctly represent the physics of the source term and make realistic assumptions on how BLEVE produce aerial overpressures. Indeed, performing time-expensive simulations of blast propagation does not mean anything if the source term is wrongly represented. Several points are still insufficiently understood and are problems for CFD attempts to simulate BLEVE. The main major problems are 1/ the liquid flashing dynamics, which follows the pressure drop and the vapour release, and involves complex homogenous and heterogeneous nucleation physics; 2/ the fluid-structure interaction, governing the opening of the vessel and therefore the vapour and flashing liquid release.
The way the flashing liquid contributes to pressure wave from BLEVE still remains a point of discussion for the scientific community. Some authors consider that the boiling of the liquid occurs infinitely fast. This means the source strength of the blast is guided only by extrinsic circumstances, which are governing the expansion of the vapour (Van den Berg, 2004). (Li et al, 2020) considered that the flashing liquid induced second phase pressure propagation with a time delay, i.e. the second phase pressure is generated after the shock wave resulted from vapour space. (Yaskush, 2016) proposed a numerical model for boil-up and expansion of two-phase mixture of superheated liquid following loss of containment. The model assumes that the mixture in the two-phase cloud stays in thermodynamic equilibrium during expansion. The author demonstrated that the

Paper Received: 15 February 2022; Revised: 9 March 2022; Accepted: 21 April 2022
Please cite this article as: Heymes F., Hoorelbeke P., Chanut C., 2022, An experimental and numerical study of the blast created by BLEVE of superheated water contained in a pipe, Chemical Engineering Transactions, 90, 103-108 DOI:10.3303/CET2290018

cloud boils up over a finite time, which makes it a less efficient ‘‘piston” for generation of blast waves due to energy release rate being limited by propagation of boiling wave through the bulk of superheated liquid. Finally, on the opposite hand, some authors consider that only the vapour phase produces a blast and believe that the liquid boiling is too slow to contribute to the pressure wave hence, the far-field blast waves are attributed to vapour expansion exclusively (Birk et al, 2020);.

The fluid-structure interaction is usually taken in account by considering that a fraction of the expansion energy is lost in mechanical rupture of the vessel. According to (Planas et al, 2004), in case of fragile failure, 80% of the energy released contributes to the creation of the pressure wave, and 40% only in case of ductile failure. In the latter case, large fragments of the vessel are propelled which explain why energy in the pressure wave is only 40%.

In fact, the reality is much more complex. A vessel containing a superheated liquid and failing will not always result in a BLEVE. In some cases, the content will be vented progressively and the hazardous consequences will remain weak (no fragments, low aerial overpressure). In other cases, a powerful explosion will entail an important aerial overpressure and eject fragments. This is due to the complex interaction between fluid and structure during BLEVE. This interaction was never considered in detail but led to a description of one-step and two-steps BLEVE (Laboureur et al, 2015). This point is particularly complex to manage in CFD, this is why the authors neglects the tank behaviour during a BLEVE.

In this work, BLEVE experiments were performed with superheated water in a tubular vessel (1D configuration). The complex dynamics of vessel rupture and opening was avoided thanks to a rupture disk that allowed a perfectly known fluid discharge opening area and little loss in ductile failure of the rupture disk. Some data about the blast are presented and CFD simulations were performed to investigate the contribution of vapour phase expansion.

2. Materials and methods

2.1 Experimental setup

The experimental materials and methods were detailed in (Heymes et al., 2019, 2020). The pressure vessel consisted in a vertical tube (internal diameter 139.76 mm, height 1064m) with a volume of 16.3L (Figure 1a).

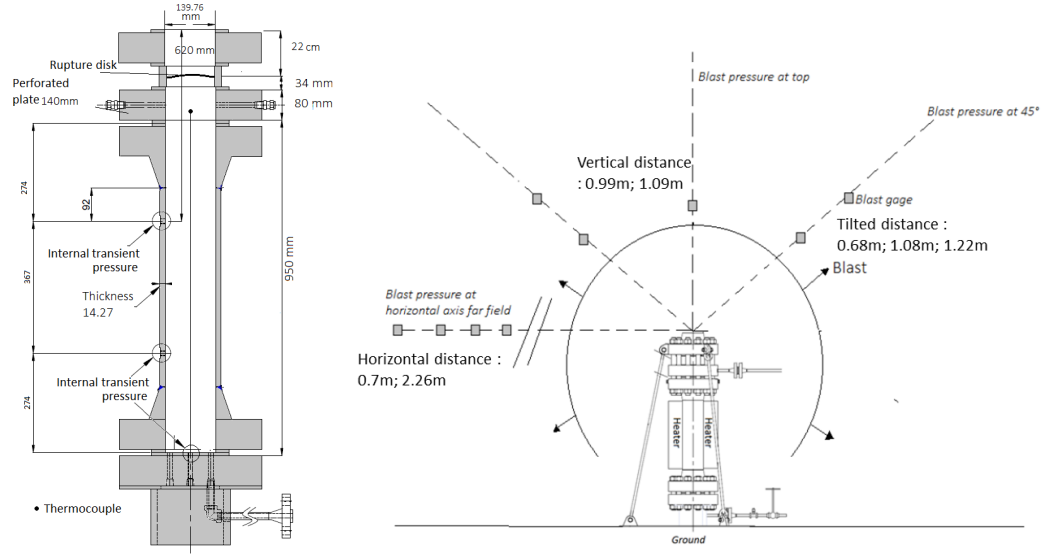

Figure 1: Experimental setup (1a, left) and location of the aerial overpressure gauges (1b, right)

The rupture disks failed at 76 bar (stainless steel 316). 27 experiments were performed by varying the initial quantity of water and the release diameter. Three high speed Internal pressure sensors (PCB M101A2) and 24 thermocouples (type K) were set in the vessel to record internal parameters. A set of 12 aerial overpressure sensors (PCB 137A23) were put on three different axis at the exit of the vessel: 4 sensors above the rupture disk on a vertical axis; 4 sensors on two 45° tilted axes pointing at the rupture disk and 4 sensors on an horizontal axis at the level of the prototype outlet. The distance between each sensor and the center of the rupture disk are given on Figure 1b. The acquisition rate was 250 kHz for pressure data (internal and aerial), and 60 Hz for temperature. The air was purged from vapor phase for each test.

2.2 CFD modelling method

CFD Modelling was performed thanks to ANSYS FLUENT software. The geometry of the cylindrical apparatus was replicated in its true dimensions and designed as bi-dimensional and axisymmetric along the axis of the prototype. Since we were only interested by the vapor release, water was considered as a solid material. Its volume was calculated by considering the thermal expansion at the rupture time. The rupture disk was represented as a surface separating the high-pressure and low-pressure domains, but without any thickness. Size of the low pressure domain was chosen to be extended 3m along the vertical axis and 3m on the radial direction, in order to avoid boundary effects. A quadrilateral method was selected for the mesh. Since the total extension of the low-pressure domain was constrained to adhere to the criteria mentioned above, three domains with different element size were created to satisfy convergence criteria and choose an opportune time step. The time step was set at 1µs, considering that the faster flow feature observed was the lead shock at about 500 $m.s^{-1}$, a spatial discretization made with elements of size Δx = 2mm give a CFL number of 0,25, which is at an available margin from the unity. According to this, a first face sizing of Δx = 2mm was chosen for the domain including the tube and above the tube opening, whereas other two face sizing of bigger dimensions were created to decrease the computational cost. The element size of the two larger grid domains was chosen in order to achieve a good quality of the mesh, having regard to aspects like skewness, smoothness and aspect ratio. The solver was density based, which is recommended for compressible, transonic flows without significant regions of low-speed flow. Solution methods chosen were density-based advection upstream splitting method (AUSM), a second order spatial discretization and a first order discretization for the time variable. For the first simulations convergence criteria were simultaneously set at 10^{-6} on each available equation. Then, to decrease the incidence of the y-velocity residual on the computational cost the choice of a lower convergence threshold (10^{-5}) was applied just for that equation. The calculation was supposed to be stopped after 25000 time-steps for a total execution time of 25ms. However, most of the simulations were interrupted before for reasons of computational cost.

3. Results and discussion

3.1 Experimental results

One test was selected for discussion. The test presented in Figure 2 was performed with 9 kg of water. The P-T state of water during heating process (1 hour) was slowly following the saturation curve until disk rupture at 76°C and 290 bar. No temperature stratification was observed excepted a cold zone at the bottom, due to a lack of heating since the lower flange avoided putting a heating collar. The temperature data (24 thermocouples) are not presented in this paper.

A first comment can be done about what happens at rupture time. The famous Reid's BLEVE theory (Reid, 1979) assumes that pressure in the vessel instantaneously reaches atmospheric pressure, entailing a high superheat level for the liquid and an explosive boiling. But the internal pressure measurement given in Figure 2b shows that this simple description is not confirmed by our experiments: the internal pressure of 76 bar drops and reaches a pseudo-stable pressure at 60 bar (during almost 15 ms), corresponding to a pressure balance driven by boiling and release dynamics. During this pressure plateau, energy is released by venting and water temperature dropps quickly. Pressure and temperature are local propagating data. The slow dynamics and inertia of thermocouples (1 mm diameter sheathed probes) doesn't allow getting data about this phenomenon at the same speed as pressure transducers, allowing plotting the actual thermodynamic state of water during pressure drop and boiling. However, Figure 2b shows that the last temperature data before disk rupture was 290°C, the following data (16 ms later) was at 140°C. We believe that the PT locus of water state during the BLEVE event never crossed the superheat limit temperature line.

Concerning aerial overpressures, there are several observations on Figure 2 c,d,e. Two pressure peaks are visible on the horizontal and tilted axis, but no second peak can be seen on the vertical axis. This is doubtless due to the vertical two-phase vapor jet which engulfed the sensors and mitigated the second pressure peak by the well know pressure wave attenuation effect of droplet clouds (see Heymes et al, 2020). Results measured on the vertical axis have to be considered carefully and will not be discussed in this paper. Concerning the double peaks on tilted and horizontal axes, the second peak is clearly weaker than the first one. The main peak during our BLEVE experiments is the first one. The impulse of the first peak is also bigger than that of the second one. This justifies why only the first peak was considered in modelling works from the literature.

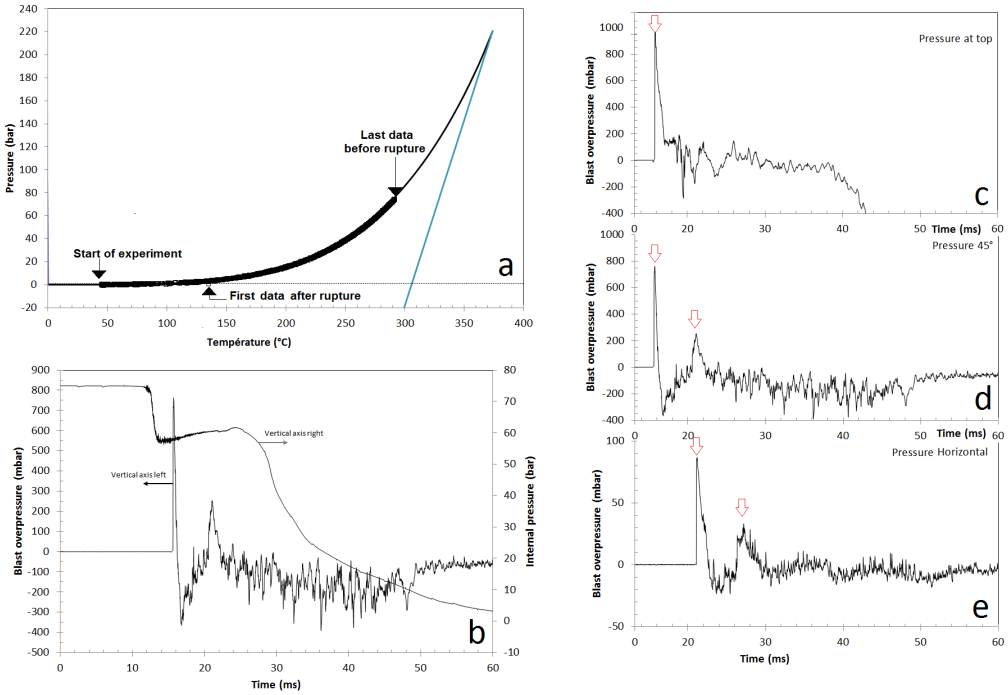

Figure 2: Data about a 9 kg water test: (a) PT plot on saturation curve; (b) Internal pressure and blast above the vessel; (c), (d) and (e) : overpressure data on the vertical axis, the tilted axis and the horizontal axis

Any pressure event happening at the internal pressure transducer will propagate to the aerial overpressure sensors by considering the propagation velocity of the pressure wave. This velocity was determined thanks to a streak image presented in (Heymes et al., 2020), and allows calculating the time shift for sensors. The analysis presented in the previously cited paper shows that the first peak is exactly produced at rupture time and corresponds therefore to the vapor expansion. Moreover, the fact that the duration of the first pressure peak is very short (0.7 ms) and stops before boiling starts indicates that boiling didn't contribute to this peak (Figure 2a). The second pressure peak is produced during the boiling process (pressure plateau on Figure 2b), but the arrival time and the duration of the pressure peak are difficult to correlate with the pressure plateau starting time and duration. It has to be noted that the propagation velocity of the second pressure peak was lower than that of the first one.

These data show that the first pressure peak seems to be only created by the vapor phase expansion; the liquid boiling could contribute to the second peak but this is not demonstrated by the results. Since CFD is able to calculated pressure propagation in gaseous phase, a CFD work was undertaken to compare the experimental data with numerical results.

3.2 Numerical results

Figure 3 shows the coloured map of pressure data at three different time steps obtained by CFD calculation. The typical mushroom shape with recirculation zones (vortex) is observed. The figure shows a very important anisotropy of the pressure, which is decreasing with distance. This is consistent with our experimental data, when comparing vertical, tilted and horizontal pressure gauges. From this data, the time evolution of pressure virtual probes located at the pressure gauges was compared with the experimental data.

Figure 4 shows experimental and numerical data obtained on the tilted axis. The tilted axis was preferred to the vertical axis since no attenuation effect of the two-phase steam jet was expected. The agreement between both curves is remarkably good with a perfect superposition of the peak, as well in intensity than in impulse. This was observed for the three distances (0.68 m; 1.08 m and 1.22 m) and confirms that the first (and main) pressure peak can be perfectly modelled by CFD by considering only the vapour phase. It has to be noted that CFD predicts a second pressure peak, with a lower intensity and following the first pressure peak. This was not observed on our experimental data.

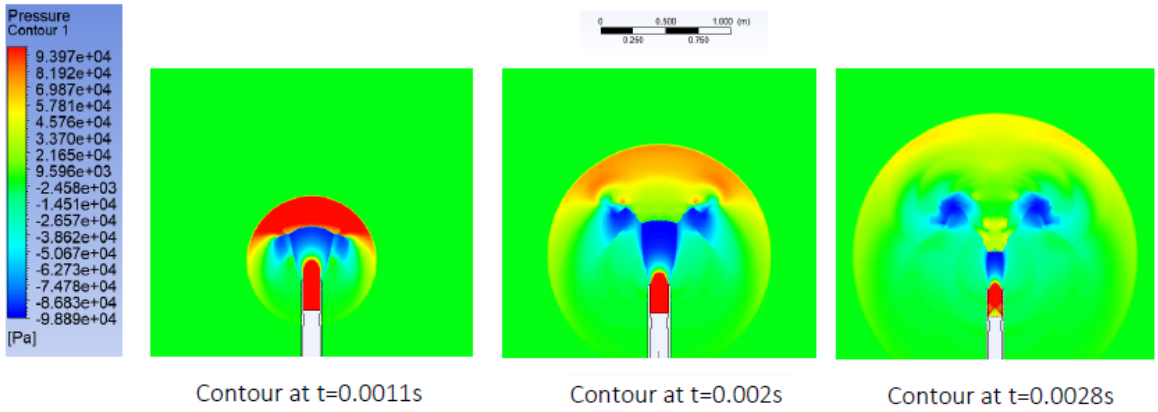

Figure 3: CFD results, mapping of overpressure

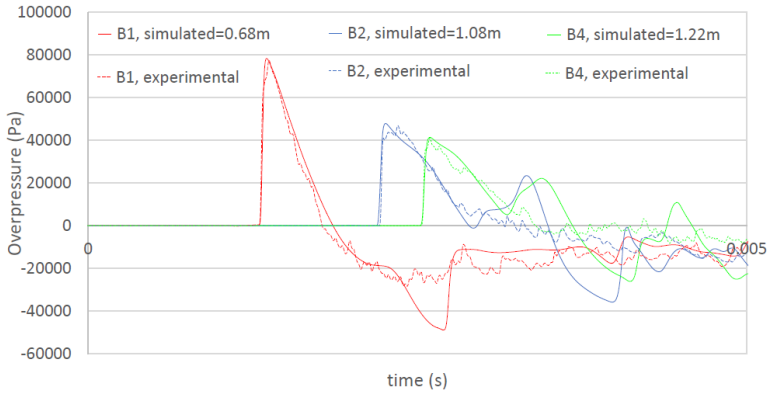

Figure 4: Comparison of experimental results with CFD simulation on the tilted axis

Aerial overpressures were also compared on the horizontal axis (0.7 and 2.26 m) in Figure 5. The experimental curve was also well predicted by the CFD results. A little error was observed for the intensity but the agreement is very good. The arrival time and impulse are also well predicted. It has to be noted that the pressure probe located at 0.7 m shows a second pressure peak, arriving 2.36 ms after the first pressure peak, and seems to correspond to a second peak calculated by CFD. This experimental pressure peak could be believed as resulting from the liquid flashing, but CFD shows that vapour expansion is also involved in this peak.

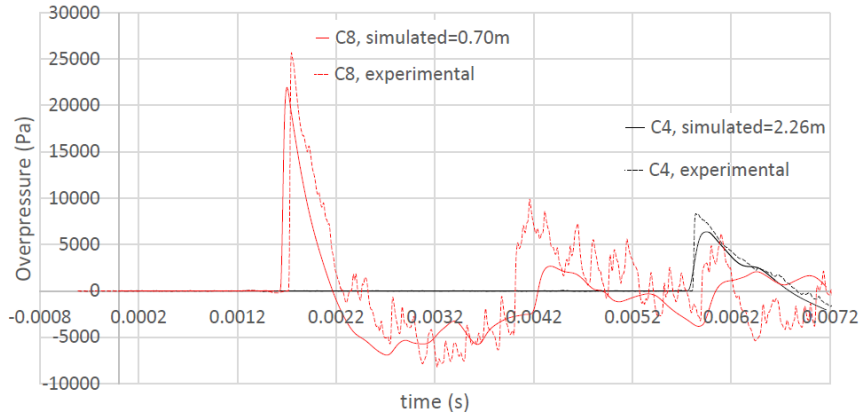

Figure 5: Comparison of experimental results with CFD simulation on the horizontal axis

4. Conclusions

This work demonstrated that CFD can reproduce perfectly the first pressure peak created by a BLEVE event. The well-defined setup and experimental data set are convenient for CFD modelling, by avoiding the tricky uncertainty about vessel rupture dynamics. This enabled demonstrating by experimental and numerical data that the first pressure peak is only due to vapour expansion. This is agreement with the recommendations of certain authors.

However, these data doesn't provide supplementary data to understand how flashing liquid could contribute to the second pressure peak. This point is currently under investigation in order to simulate the pressure drop, the vaporization wave, the two-phase mixture expansion and the piston effect that could produce a second blast.

A concern about this work is that this 1D experimental campaign may not be exactly what happens during a 3D tank BLEVE. This question is difficult to answer, since the current lack of knowledge about fluid-structure reciprocal interaction during a BLEVE doesn't provide arguments to help. The liquid flashing could be more intense in case of total destruction of a vessel, and could create a bigger pressure wave. This is also a current point of investigation in our work.

Acknowledgments

The authors are grateful to Total SA for supporting this research work, to the Institute for Risk Science team (namely Zacaria Essaidi, Christian Lopez, Laurent Aprin, Florian Dizier and Roland Eyssette for their help during the testing campaign, and the Camp des Garrigues military camp for access to the facility.

References

Birk A.M., Cunningham, H., 1994, The boiling expanding vapour explosion, Journal of Loss Prevention in the Process Industries, Volume 7, Pages 474-480.

Birk A.M., Eyssette R., Heymes F., 2020, Analysis of BLEVE overpressure using spherical shock theory,
Process Safety and Environmental Protection, Volume 134, Pages 108-120,

Birk A.M., Heymes F., Eyssette R., Lauret P., Aprin L., Slangen P., 2018, Near-field BLEVE overpressure effects: The shock start model, Process Safety and Environmental Protection, Volume 116, Pages 727-736

Hansen, O.R., Kjellander, M.T., 2016, CFD modelling of blast waves from BLEVEs, Chemical Engineering Transactions, Volume 48, 199-204.

Heymes, F., Lauret, P., Hoorelbeke, P., 2019, An Experimental Study of Water BLEVE, Chemical Engineering Transactions, Volume 77, 205-210.

Heymes, F., Lauret, P., Hoorelbeke, P., 2020, An Experimental Study of Water BLEVE, Process Safety and Environmental Protection, Volume 141, Pages 49-60

Laboureur D., Birk A.M., Buchlin J.M., Rambaud P., Aprin L., Heymes F., Osmont A., 2015, A closer look at BLEVE overpressure, Process Safety and Environmental Protection, Volume 95, 159–171.

Li J., Hao, H., Numerical study of medium to large scale BLEVE for blast wave prediction, Journal of Loss Prevention in the Process Industries, Volume 65, 2020

Li J., Hao H., 2021, Numerical simulation of medium to large scale BLEVE and the prediction of BLEVE's blast wave in obstructed environment, Process Safety and Environmental Protection, Volume 145, Pages 94-109,

Planas-Cuchi, E., Salla, J.M., Casal, J., 2004, Calculating overpressure from BLEVE explosions, Journal of Loss Prevention in the Process Industries, Volume 17, 431–436.

Reid R.C., 1979, Possible mechanism for pressurized-liquid tank explosions or BLEVE's, Science, Volume 203, 1263–1265.

Van den Berg, A.C., van der Voort, M.M., Weerheijm, J., Versloot, N.H.A., 2004, Expansion-controlled evaporation: a safe approach to BLEVE blast, Journal of Loss Prevention in the Process Industries, Volume 17, 397–405.

Yakush S.E., 2016, Model for blast waves of Boiling Liquid Expanding Vapor Explosions, International Journal of Heat and Mass Transfer, Volume 103,173-185